Article

Cell Reports

Forebrain *Ptf1a* Is Required for Sexual Differentiation of the Brain

Graphical Abstract

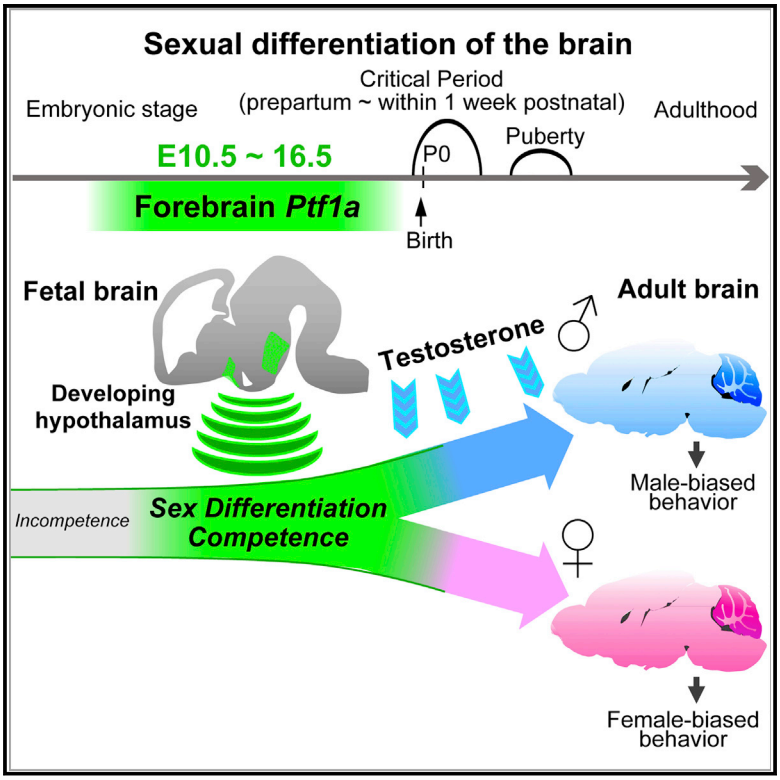

Highlights

- Ptf1a is expressed near the ventricular zone in the developing hypothalamus at E10–E16
- *Ptf1a* cKO male and female mice lose sex-biased behaviors and gene expression
- Kisspeptin neuron development is severely disrupted in *Ptf1a*-deficient hypothalamus
- RNA-seq analysis reveals altered gene expression in non-cell-autonomous regulators

Authors

Tomoyuki Fujiyama, Satoshi Miyashita, Yousuke Tsuneoka, ..., Masashi Yanagisawa, Hiromasa Funato, Mikio Hoshino

Correspondence

funato.hiromasa.km@u.tsukuba.ac.jp (H.F.), hoshino@ncnp.go.jp (M.H.)

In Brief

Fujiyama et al. find that forebrain-specific *Ptf1a*-deficient mice (*Ptf1a* cKO) exhibit abnormalities in sexually dimorphic behaviors, reproductive organs, and severely altered expression of sex-biased genes, including *Kiss1*, in the hypothalamus in both sexes, which suggests that forebrain *Ptf1a* is one of the earliest regulators for sexual differentiation of the brain.

Data and Software Availability

GSE112935

Fujiyama et al., 2018, Cell Reports *24*, 79–94
July 3, 2018 © 2018 The Authors.
https://doi.org/10.1016/j.celrep.2018.06.010

CellPress

Cell Reports
Article

OPEN ACCESS
CellPress

Forebrain *Ptf1a* Is Required for Sexual Differentiation of the Brain

Tomoyuki Fujiyama,[1,2] Satoshi Miyashita,[1] Yousuke Tsuneoka,[5] Kazumasa Kanemaru,[3] Miyo Kakizaki,[2] Satomi Kanno,[2] Yukiko Ishikawa,[2] Mariko Yamashita,[1,6] Tomoo Owa,[1] Mai Nagaoka,[1] Yoshiya Kawaguchi,[7] Yuchio Yanagawa,[8] Mark A. Magnuson,[9] Masafumi Muratani,[4] Akira Shibuya,[3] Yo-ichi Nabeshima,[10] Masashi Yanagisawa,[2] Hiromasa Funato,[2,5,*] and Mikio Hoshino[1,11,*]

[1]Department of Biochemistry and Cellular Biology, National Institute of Neuroscience, NCNP, Kodaira, Tokyo 187-8502, Japan
[2]International Institute for Integrative Sleep Medicine (WPI-IIIS), University of Tsukuba, Tsukuba, Ibaraki 305-8575, Japan
[3]Department of Immunology, University of Tsukuba, Tsukuba, Ibaraki 305-8575, Japan
[4]Department of Genome Biology, University of Tsukuba, Tsukuba, Ibaraki 305-8575, Japan
[5]Department of Anatomy, Toho University, Tokyo 143-8540, Japan
[6]Department of Developmental and Regenerative Biology, Tokyo Medical and Dental University, Tokyo 113-8510, Japan
[7]Center for iPS Cell Research and Application, Kyoto University, Kyoto 606-8507, Japan
[8]Department of Genetic and Behavioral Neuroscience, Gunma University, Maebashi 371-8511, Japan
[9]Department of Cell and Developmental Biology, Vanderbilt University Medical Center, Nashville, TN 37232, USA
[10]Foundation for Biomedical Research and Innovation, Kobe 650-0047, Japan
[11]Lead Contact
*Correspondence: funato.hiromasa.km@u.tsukuba.ac.jp (H.F.), hoshino@ncnp.go.jp (M.H.)
https://doi.org/10.1016/j.celrep.2018.06.010

SUMMARY

The mammalian brain undergoes sexual differentiation by gonadal hormones during the perinatal critical period. However, the machinery at earlier stages has not been well studied. We found that *Ptf1a* is expressed in certain neuroepithelial cells and immature neurons around the third ventricle that give rise to various neurons in several hypothalamic nuclei. We show that conditional *Ptf1a*-deficient mice (*Ptf1a* cKO) exhibit abnormalities in sex-biased behaviors and reproductive organs in both sexes. Gonadal hormone administration to gonadectomized animals revealed that the abnormal behavior is caused by disorganized sexual development of the knockout brain. Accordingly, expression of sex-biased genes was severely altered in the cKO hypothalamus. In particular, *Kiss1*, important for sexual differentiation of the brain, was drastically reduced in the cKO hypothalamus, which may contribute to the observed phenotypes in the *Ptf1a* cKO. These findings suggest that forebrain *Ptf1a* is one of the earliest regulators for sexual differentiation of the brain.

INTRODUCTION

Male and female brains exhibit various sex differences in their structures and functions. It is well known that sexual differentiation of the brain is determined largely by the levels of gonadal steroid hormones during the perinatal critical period (Bonthuis et al., 2010; McCarthy and Arnold, 2011; Yang and Shah, 2014). Perinatal exposure of high levels of testosterone induces masculinization of the brain independent of genetic sex, whereas the blockade of androgen during the critical period in male animals suppresses masculinization of the brain (Bonthuis et al., 2010). However, the mechanisms prior to the critical period are not well understood.

The hypothalamus is one of the brain regions responsible for sex dimorphism. It is a forebrain structure composed of diverse groups of nuclei as well as neurons and is involved in the homeostatic regulation of body weight, energy metabolism, and sleep and wakefulness via hormonal and autonomic systems (Sternson, 2013). The hypothalamus contains several sexually dimorphic nuclei, such as the medial preoptic area (MPOA), ventromedial nucleus (VMH), and arcuate nucleus (ARH), that regulate sex-biased behaviors (e.g., sexual behavior, aggression, parenting), and gonadal hormones via the hypothalamic-pituitary-gonadal (HPG) axis (d'Anglemont de Tassigny and Colledge, 2010; Tsuneoka et al., 2013; Anderson, 2016; Forger et al., 2016).

Hypothalamic development progresses through several stages composed of regionalization, neuronal stem cell proliferation, neuronal differentiation, and migration that are governed by a spatiotemporal network of transcription factors (Shimogori et al., 2010; Morales-Delgado et al., 2011; Bedont et al., 2015; Xie and Dorsky, 2017). Loss-of-function experiments have proven the essential roles of transcription factors in the formation of hypothalamic subregions and the induction of specific neuronal subtypes and subsequent proper function of the hypothalamus. For example, a functional deficiency in a basic-helix-loop-helix (bHLH) transcription factor, Sim1, disturbs proper formation of the paraventricular hypothalamic nucleus and differentiation of neurons expressing oxytocin, vasopressin, corticotropin-releasing hormone, and thyrotropin-releasing hormone (Michaud et al., 1998). In addition, Sim1 haploinsufficiency causes obesity (Hossain et al., 2016). Although many loss-of-function studies for transcription factors in the hypothalamus have been done, altered sexual differentiation of the brain has not been reported.

This is an open access article under the CC BY license (http://creativecommons.org/licenses/by/4.0/).

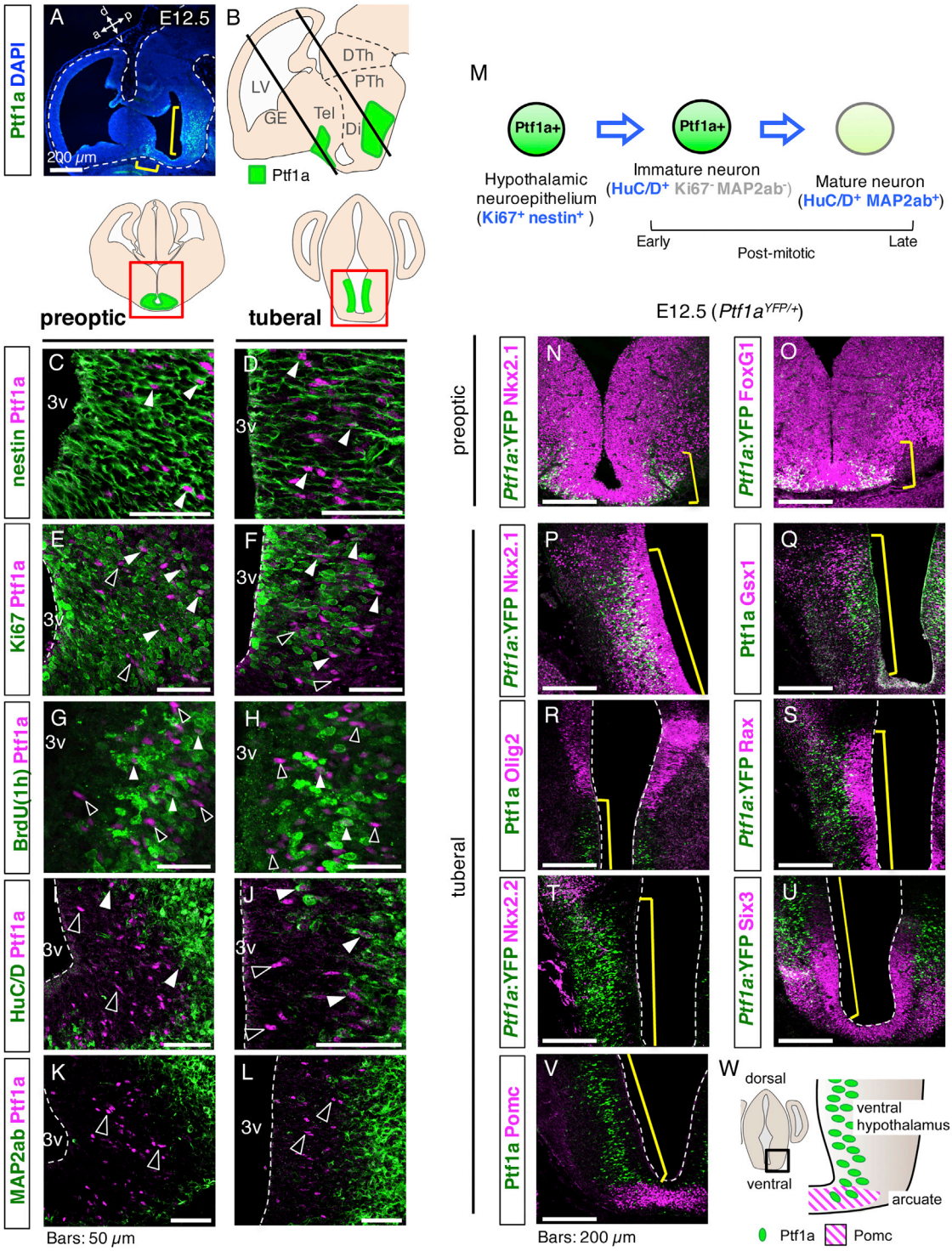

Figure 1. Ptf1a Expression in the Developing Forebrain

Double labeling with Ptf1a and a marker in the wild-type hypothalamus at E12.5.

(A) Sagittal section. Yellow brackets indicate the Ptf1a-positive regions. A montage of four original images.

(B) Schematic diagrams of Ptf1a expression regions (green). Black lines indicate the level of sections for preoptic and tuberal regions. See also Figure S1.

(C–L) Coronal sections of preoptic (C, E, G, I, and K) and tuberal (D, F, H, J, and L) regions. White arrowheads indicate double-positive cells for Ptf1a and the marker, whereas hollow arrowheads highlight Ptf1a-single-positive cells.

(legend continued on next page)

Some hypothalamic genes and proteins have been reported to be differentially expressed in males and females. Among them are kisspeptin, calbindin, and estrogen receptor (Semaan and Kauffman, 2010; Forger et al., 2016; Tsuneoka et al., 2017). Kisspeptin, a neuropeptide produced from the *Kiss1* gene, is expressed in neurons of the anteroventral periventricular nucleus (AVPV) and ARH. Because kisspeptin expression is detected as early as embryonic day (E) 13.5 in the ARH (Knoll et al., 2013) and because loss-of-function mutations of this gene and its receptor GPR54 result in disturbed sexual differentiation of the brain (Kauffman et al., 2007; Nakamura et al., 2016), kisspeptin signaling may play an important role in sexual development of the brain, putatively at embryonic stages. However, the machinery upstream of kisspeptin signaling has not been well studied. Moreover, it is still unclear whether there are other pathways to regulate brain sex differentiation.

Pancreas transcription factor 1a (*Ptf1a*) is a bHLH transcription factor that plays important roles in the development of all cerebellar GABAergic neurons (Hoshino et al., 2005), GABAergic and glycinergic inhibitory neurons in the cochlear nucleus, climbing fiber neurons in the inferior olivary nucleus (Yamada et al., 2007; Fujiyama et al., 2009), inhibitory neurons in the spinal cord dorsal horn (Glasgow et al., 2005), and amacrine and horizontal cells in the retina (Fujitani et al., 2006). Although *Ptf1a* is expressed in the developing forebrain (Meredith et al., 2009), the forebrain role of *Ptf1a* has not been examined.

In the present study, we show that Ptf1a is expressed in neuroepithelial cells and immature neurons around the ventricular zone of the preoptic and tuberal regions and that a number of *Ptf1a*-lineage cells are found in the MPOA, VMH, and ARH in adulthood. Mice deficient in forebrain *Ptf1a* exhibit abnormal sex-biased behaviors and maldevelopment of sexual dimorphism in the brain and reproductive organs. Loss of *Kiss1* at E14.5 was one of the earliest changes found in the *Ptf1a*-deficient mice. We observed two types of phenotypes in the conditional knockout (cKO) mice, Kiss1-dependent and Kiss1-independent. RNA sequencing (RNA-seq) analysis using cells sorted by fluorescence-activated cell sorting (FACS) expressed *Ptf1a* from E14.5 brains showed significant changes in gene expression, some of which are thought to account for both types of phenotypes. These findings suggest that Ptf1a is involved in proper sexual differentiation of the brain and further suggest that the events leading to brain sexual development occur even before the critical period.

RESULTS

Expression of *Ptf1a* in the Developing Hypothalamus

We performed immunostaining for Ptf1a in the developing forebrain. Ptf1a-positive cells were observed from E10.5 to E16.5 in the ventricular zone of the preoptic area and tuberal region (Figures 1A, 1B, and S1). The density of Ptf1a-positive cells peaked at E12.5–E14.5 (Figures S1A–S1E), and positive cells were rarely observed after E16.5 (Figures S1F and S1G). At E12.5, Ptf1a-positive cells were co-labeled with nestin (Figures 1C and 1D) and a proliferative marker, Ki67 (Figures 1E and 1F). One hour after the injection of BrdU, we observed BrdU-incorporated Ptf1a-positive cells (S-phase cells; Figures 1G and 1H). Whereas some Ptf1a-positive cells were co-labeled with an early neuronal marker, HuC/D, no Ptf1a-positive cells were positive for a mature neuron marker, MAP2ab (Figures 1I–1L). This indicates that Ptf1a is expressed in dividing neuroepithelial cells and early postmitotic neurons but not in mature neurons (Figure 1M).

Next, we examined where the *Ptf1a*-positive cells were located in the developing hypothalamus of *Ptf1a*^{YFP} heterozygous embryos in which we observed Ptf1a-positive cells in both the ventricular and mantle zones, likely due to the longer half-life of YFP compared with Ptf1a protein. Consistent with the immunostaining for Ptf1a, *Ptf1a*-YFP cells in the preoptic level were co-labeled with FoxG1 and Nkx2.1, which are expressed in the developing preoptic area (Figures 1N and 1O) (Shimogori et al., 2010). In the tuberal region, the *Ptf1a*-positive cells were distributed within the region expressing Nkx2.1 (Figure 1P) and Gsx1 (Figure 1Q) (Shimogori et al., 2010; Lee et al., 2016), whereas the *Ptf1a* expression region did not overlap with prethalamic region expressing Olig2 (Figure 1R) (Shimogori et al., 2010). The dorsal end of the *Ptf1a* expression region corresponded to that of the Rax expression region (Figure 1S) and was adjacent to the ventral end of the Nkx2.2 expression region (Figure 1T). There were fewer *Ptf1a* positive cells in the ventral end of the tuberal region that expressed Six3 (Figure 1U) and Pomc (Figure 1V) (Shimogori et al., 2010). Thus, the tuberal *Ptf1a* expression region occupies the diencephalic ventral region with the exception of the ventralmost region (Figure 1W).

Fate Mapping of Hypothalamic *Ptf1a*-Lineage Cells

To investigate cell fates of hypothalamic *Ptf1a*-lineage cells, we visualized *Ptf1a*-lineage cells in adult brains of *Ptf1a*$^{cre/+}$; *Rosa26*^{LacZ} mice. X-gal signals were strongly observed in the preoptic area and tuberal region (Figures 2A–2D). In the preoptic area, many X-gal-positive cells were observed in the MPOA, including the AVPV, whereas no signals were observed in the median preoptic area or lateral preoptic area. In the tuberal region, X-gal-positive cells were abundant in the VMH, dorsomedial nucleus (DMH), and ARH, whereas a few X-gal-positive cells were scattered in the lateral hypothalamic area, median eminence, and medial tuberal nucleus. No X-gal-positive cells were observed in the paraventricular hypothalamic nucleus, suprachiasmatic nucleus, or anterior hypothalamus (Table S1).

Staining for β-gal combined with immunostaining for cell-type markers revealed that almost all of the *Ptf1a*-lineage cells were

(M) Schematic diagram of Ptf1a expression in the developing hypothalamus. Ptf1a-positive cells are in cell cycling state (nestin$^+$, Ki67$^+$) and early postmitotic phase (HuC/D$^+$, Ki67$^-$, MAP2ab$^-$). Ptf1a expression disappears in mature neurons.
(N–V) Coronal sections of preoptic (N and O) and tuberal (P–V) regions. Yellow brackets indicate the range of *Ptf1a* expression.
(W) Schematic of the ventro-tuberal *Ptf1a* expression with Pomc expression region.
Di, diencephalon; DTh, dorsal thalamus; GE, ganglionic eminence; LV, lateral ventricle; PTh, prethalamus; Tel, telencephalon; 3v, third ventricle.
Scale bars in (C)–(L), 50 μm; scale bars in (N)–(W), 200 μm. See also Figure S1.

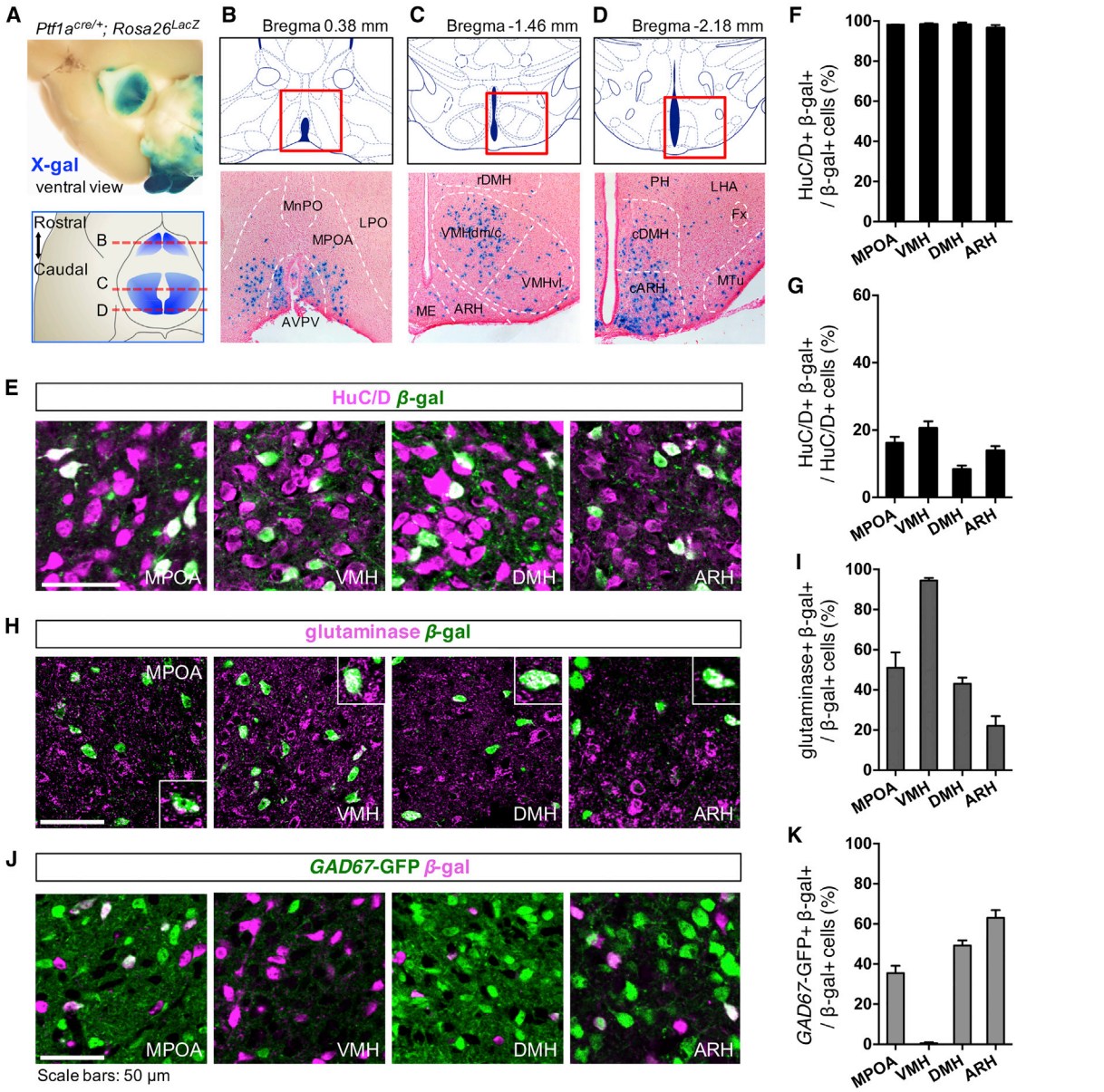

Figure 2. Fate Mapping and Characterization of *Ptf1a*-Lineage Cells in the Adult Hypothalamus

(A) Ventral view of whole-mount X-gal stained adult brain of *Ptf1a*$^{cre/+}$; *Rosa26*^{LacZ} and a schematic distribution of *Ptf1a*-lineage cells in the hypothalamus.

(B–D) Coronal sections at the level of dashed lines in (A). X-gal labeled cells are located in the ventrobasal hypothalamus including MPOA (B), VMH, DMH, and ARH (C and D). Region of interest is indicated by red rectangle in upper schematic. Magnified views are serially represented. Sections are counterstained with Nuclear Fast Red.

(E, H, and J) Double staining with β-gal and a marker (HuC/D in E, glutaminase in H, and *GAD67*-GFP in J) in the indicated hypothalamic regions (MPOA, VMH, DMH, ARH) of the *Ptf1a*$^{cre/+}$; *Rosa26*^{LacZ} adults. Insets in (H): magnified views of double-positive cells are shown. Scale bars, 50 μm.

(F) HuC/D-positive cells scored as a percentage of the β-gal-positive cells (n > 100 cells from two to four independent mice for each region). See also Figure S2.

(G) The percentages of β-gal-positive cells in HuC/D-positive neurons (n > 600 cells from two to four mice for each region).

(I and K) Quantification of glutaminase (I) or *GAD67*-GFP (K) co-labeling in β-gal-positive cells. Bars indicate the percentage of co-labeling among *Ptf1a*-lineage cells expressing detectable levels of the neurotransmitter subtype marker.

AVPV, anteroventral periventricular nucleus; cARH, caudal ARH; cDMH, caudal DMH; Fx, fornix; LHA, lateral hypothaalmic area; LPO, lateral preoptic area; ME, median eminence; MnPO, median preoptic area; MPOA, medial preoptic area; MTu, medial tuberal nucleus; PH, posterior hypothalamic area; rDMH, rostral DMH; VMHc, central; VMHdm, dorsomedial; VMHvl, ventrolateral part of VMH.

Data are expressed as mean ± SEM. Experimental values represent the averages of at least two independent mice. See also Figure S2 and Table S1.

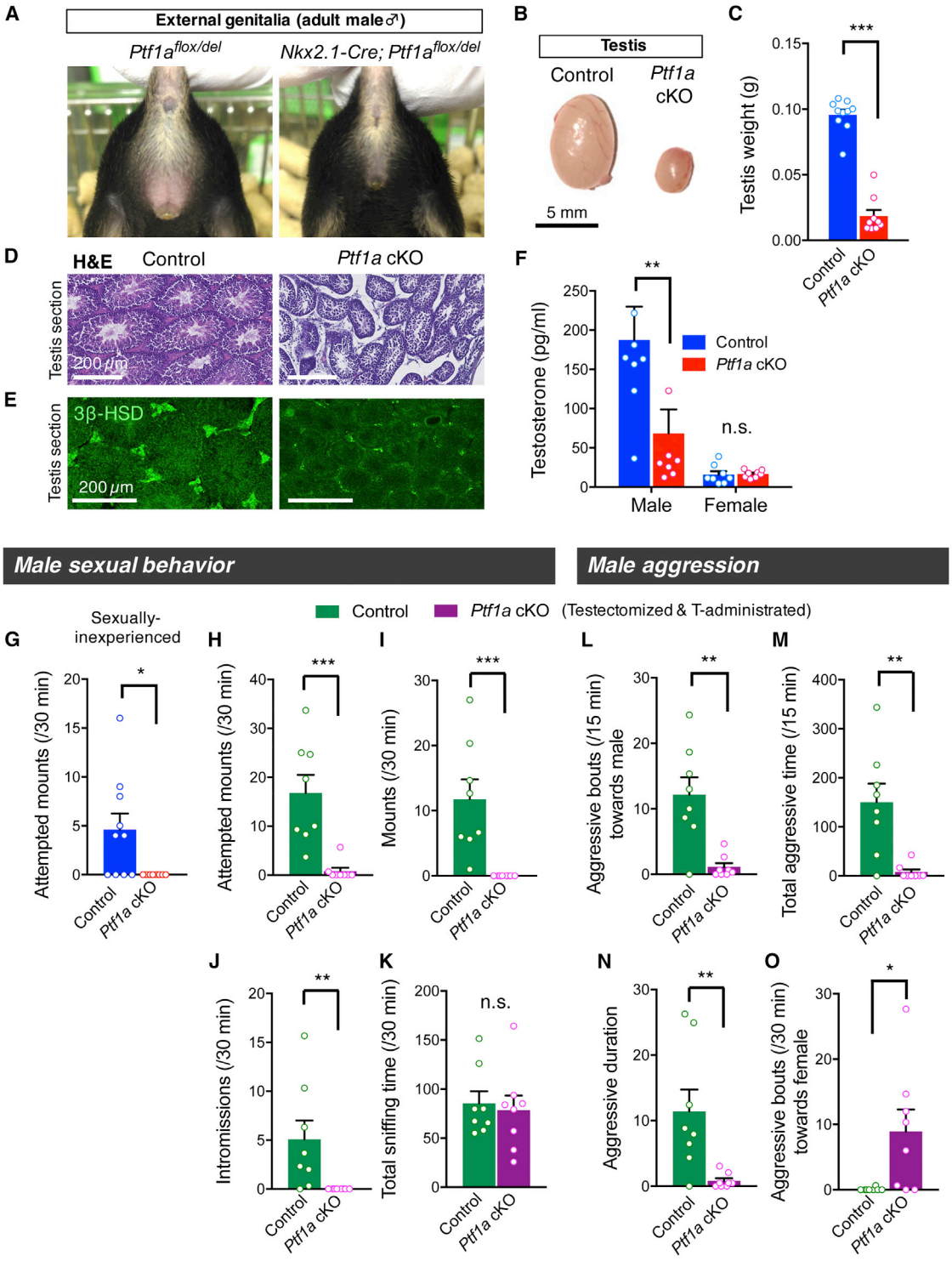

Figure 3. Gonadal Development and Sexually Biased Behaviors Were Impaired in Hypothalamic *Ptf1a*-Deficient Adult Male Mice

Male mice lacking forebrain Ptf1a display sexual immaturity phenotypes, including micropenis, reduced testis size, decreased blood testosterone, and sexually biased behaviors.

(A) External genitalia of *Ptf1a* cKO and control male mice at 4–5 weeks of age.

(B) Representative images of testis from control and *Ptf1a* cKO male mice.

(C) Quantification of testis weights (n = 9 mice per group). Circles indicate individual scores. Mann-Whitney U test.

(D) Representative images of H&E staining of testis from control and *Ptf1a* cKO mice. No signs of spermatogenesis in testes from *Ptf1a* cKO mice.

(legend continued on next page)

positive for a neuronal marker, HuC/D, in the adult hypothalamus (MPOA, 98.2 ± 0.02%; VMH, 98.3 ± 0.57%; DMH, 98.2 ± 1.15%; ARH, 96.5 ± 1.44%; Figures 2E and 2F). We did not observe any *Ptf1a*-lineage cells co-labeled with an astrocytic marker, glial fibrillary acidic protein (GFAP), or an oligodendrocyte lineage marker, NG2 (Figures S2A and S2B). *Ptf1a*-lineage cells accounted for 16.3 ± 1.7%, 20.6 ± 2.1%, 8.3 ± 1.2%, and 13.8 ± 1.4% of neurons in the MPOA, VMH, DMH and ARH, respectively (Figure 2G). In the MPOA and DMH, approximately 50% of the *Ptf1a*-lineage cells were co-labeled with a glutamatergic neuron marker glutaminase (Figures 2H and 2I), whereas 40%–50% of the *Ptf1a*-lineage cells were visualized by the presence of *GAD67*-GFP (Tamamaki et al., 2003) (Figures 2J and 2K), indicating that the hypothalamic *Ptf1a* expression regions produced both excitatory and inhibitory neurons. Consistent with the fact that the VMH rarely contains GABAergic neurons, almost all of the *Ptf1a*-lineage cells in the VMH were positive for glutaminase (Figure 2I). Approximately 60% of the *Ptf1a*-lineage cells were GABAergic neurons in the ARH which contains abundant GABAergic neurons (Figure 2K).

Forebrain *Ptf1a*-Lineage Cells in *Ptf1a*-Null Mice

Next, we examined whether *Ptf1a* deficiency affects the migration and survival of forebrain *Ptf1a*-lineage cells. The distribution and size of *Ptf1a*-lineage areas in the preoptic and tuberal regions of $Ptf1a^{cre/del}$; $Rosa26^{LacZ}$ mice were similar to those of $Ptf1a^{cre/+}$; $Rosa26^{LacZ}$ mice (Figure S3A). The numbers of *Ptf1a*-lineage cells were similar between $Ptf1a^{cre/del}$; $Rosa26^{EYFP/+}$ and $Ptf1a^{cre/+}$; $Rosa26^{EYFP/+}$ mice at E18.5 (Figures S3B and S3C). Thus, loss of Ptf1a did not affect survival and migration of *Ptf1a*-lineage cells. Consistently, there was no difference in the number of cells positive for an apoptotic cell death marker, Caspase3A, between $Ptf1a^{cre/del}$ and $Ptf1a^{cre/+}$ embryos (Figures S3D and S3E). In addition, the majority of *Ptf1a*-lineage cells in the VMH were *GAD67*-GFP negative in *Ptf1a*-null mice (Figure S3F), suggesting no overt change in the excitatory versus inhibitory cell fate, unlike as reported in the retina and spinal cord in *Ptf1a*-null mice (Glasgow et al., 2005; Fujitani et al., 2006).

Abnormal Genitalia and Sexual Behaviors in Forebrain *Ptf1a*-Deficient Adult Male Mice

To conditionally inactivate *Ptf1a*, we generated $Ptf1a^{flox}$ mice in which the entire Ptf1a-coding region was flanked by two loxP sequences (Figures S4A–S4C). Consistent with En1 expression in the mesencephalon and rhombomere 1 (Kimmel et al., 2000), $En1^{Cre/+}$; $Ptf1a^{flox/flox}$ mice were completely lacking in cerebellar structure (Figure S4D), as previously reported (Hoshino et al., 2005), confirming the Cre-dependent disruption of *Ptf1a* in $Ptf1a^{flox/flox}$ mice. To disrupt *Ptf1a* in the forebrain, we used *Nkx2.1-Cre* mice because Nkx2.1 is expressed in *Ptf1a* expression regions in both the preoptic and tuberal regions (Figures 1N and 1P) but not in the hindbrain or spinal cord. As predicted, *Nkx2.1-Cre*; $Ptf1a^{flox/YFP}$ mice lacked Ptf1a-positive cells in both the preoptic and tuberal *Ptf1a* expression regions (Figures S4E and S4F).

Forebrain-specific *Ptf1a*-deficient mice (*Ptf1a* cKO mice) were generally healthy but infertile. Male *Ptf1a* cKO mice had a small penis and undescended and very small testes (Figures 3A–3C). The testes of *Ptf1a* cKO mice had thin seminiferous tubules containing only spermatogonia, but not spermatids or sperm (Figure 3D), suggesting a total lack of spermatogenesis. Immunostaining for 3β-HSD revealed a massive reduction in Leydig cells (Figure 3E). Serum testosterone levels were significantly lower in *Ptf1a* cKO male mice than in control mice (Figure 3F). *Ptf1a* cKO mice did not exhibit any mounting behavior toward a female mouse (Figure 3G).

Masculinization of the adult brain can be assessed by the male sexual behaviors induced by testosterone (Yang and Shah, 2014). We therefore observed sexual behaviors of castrated *Ptf1a* cKO mice supplemented with testosterone. *Ptf1a* cKO mice did not exhibit sexual behaviors in response to testosterone compared with control littermates, despite no difference in sniffing between *Ptf1a* cKO and control mice (Figures 3H–3K). Furthermore, whereas testosterone supplementation in male control mice induced aggression toward a same-sex mouse, male *Ptf1a* cKO mice rarely exhibited aggressive behavior toward other male mice (Figures 3L–3N). Interestingly, testosterone-supplemented *Ptf1a* cKO mice exhibited frequent incidences of aggression toward a female mouse, which was rarely observed in male control mice (Figure 3O). Thus, male *Ptf1a* cKO mice did not exhibit male-typical behaviors related to masculinized brains.

Abnormal Genitalia and Sexual Behaviors in the *Ptf1a*-Deficient Adult Female Mice

Fertility tests confirmed that female *Ptf1a* cKO mice were infertile (data not shown). Female *Ptf1a* cKO mice exhibited a thin uterus (Figure 4A) and a complete lack of corpus lutea in their ovaries (Figure 4B). The weight of the ovaries and serum 17β-estradiol levels in female *Ptf1a* cKO mice were similar to those of control female mice (Figures 4C and 4D). Furthermore, female *Ptf1a* cKO mice did not exhibit an estrous cycle, instead remaining in the diestrus state (Figures 4E–4G). These results indicated that the gonadal function of female *Ptf1a* cKO mice was severely disrupted.

(E) Anti-3β-HSD antibody immunostaining for Leydig cells in testis of control and *Ptf1a* cKO mice.
(F) Serum testosterone levels of *Ptf1a* cKO mice and control mice (n = 8 per group). One-way ANOVA followed by Tukey's test.
(G) Quantification of mounting behavior toward female in virgin *Ptf1a* cKO and control male mice (n = 10 per group). Circles represent individual trials. Mann-Whitney U test.
(H–K) Male sexual behaviors were scored in testectomized and testosterone-supplemented *Ptf1a* cKO and control male mice (n = 8 per group). Attempted mounts (H), mounts (I), intromissions (J), and total sniffing time (K) are shown. Mann-Whitney U test.
(L–O) Male aggression behaviors were scored in *Ptf1a* cKO and control male mice (n = 8 per group). Aggressive bouts towards male (L), total aggressive time (M), aggressive duration (N), and aggressive bouts towards female (O) are shown. Mann-Whitney U test.
Data are expressed as mean ± SEM. *$p < 0.05$, **$p < 0.01$, and ***$p < 0.001$. In (C) and (F), each individual circle value is a mean of two independent biological replicates. In (H)–(O), each circle value is a mean of three independent replicates. See also Figures S4 and S5.

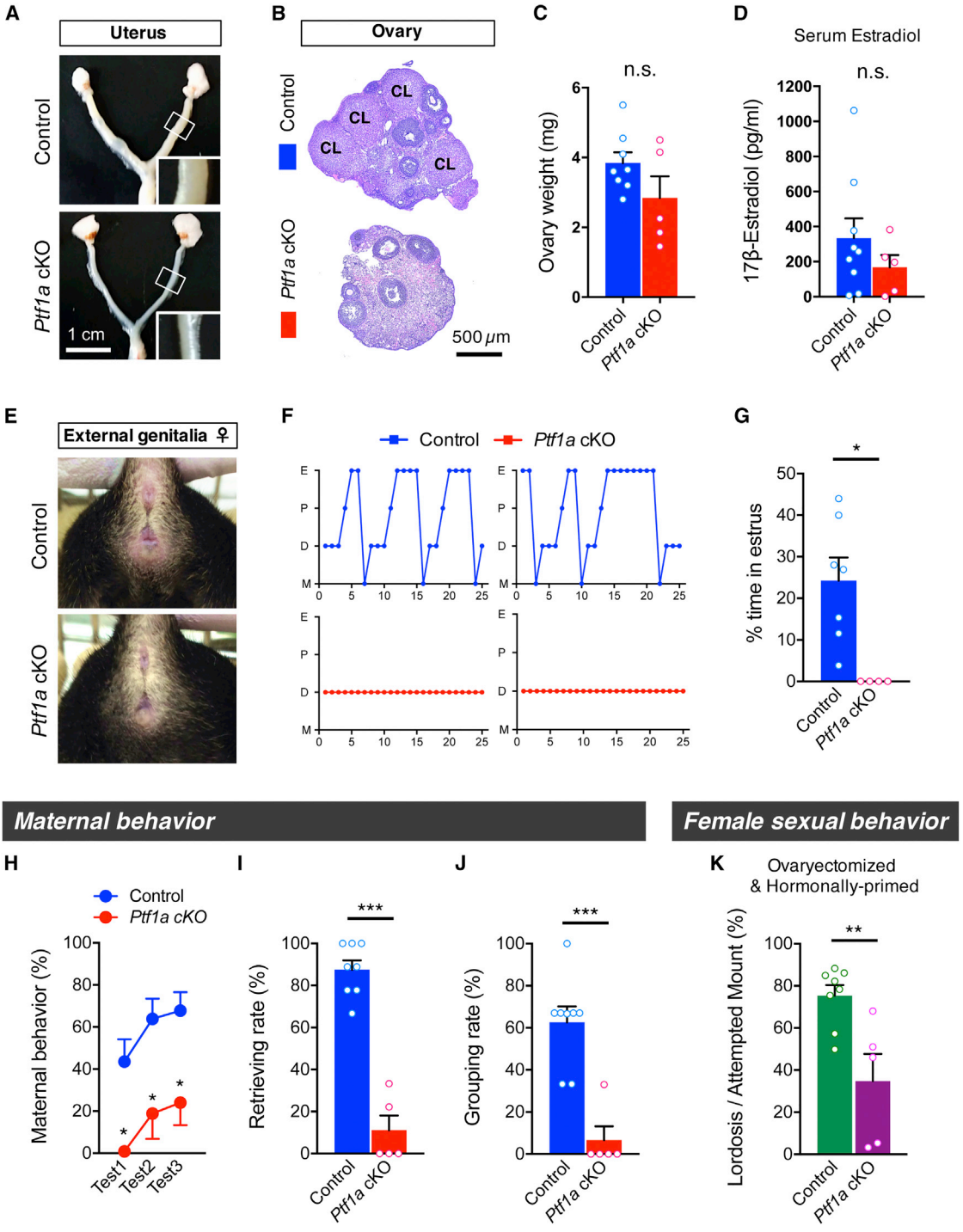

Figure 4. Gonadal Development and Sexually Biased Behaviors Were Impaired in Hypothalamic *Ptf1a*-Deficient Adult Female Mice

(A) Representative images of uterus from adult *Ptf1a* cKO and control mice. Magnified views of boxed region are showed in insets.

(B) Ovarian histology in adult *Ptf1a* cKO and control mice. Corpora lutea (CL) were observed in control mice but missing in *Ptf1a* cKO mice (n = 4 mice per group).

(C and D) No significant changes in ovary weights (C; control, n = 8; *Ptf1a* cKO, n = 5) or serum 17β-estradiol levels (D; control, n = 9; *Ptf1a* cKO, n = 5). Student's t test.

(E) Images of external genitalia in *Ptf1a* cKO and control female mice.

(F) Representative adult estrous cycle profiles for two control (top) and two *Ptf1a* cKO (bottom) female mice.

(G) The percentage of time spent in estrus in control (n = 7) and *Ptf1a* cKO (n = 4) mice. Student's t test.

(legend continued on next page)

Next, we examined maternal behaviors of virgin female *Ptf1a* cKO mice (Tsuneoka et al., 2013). *Ptf1a* cKO mice displayed significantly fewer maternal behaviors, including nest building, crouching, licking, retrieving, and grouping pups into the nest, than control female mice (Figures 4H–4J). Furthermore, whereas pretreatment with estrogen and progesterone induced the lordosis reflex in ovariectomized control mice, the same pretreatment induced fewer instances of the lordosis reflex in ovariectomized *Ptf1a* cKO mice (Figure 4K).

Altered Sex Differences in Metabolism in the *Ptf1a*-Deficient Female Mice

In addition to sexual behaviors, C57BL/6 mice show sex differences in energy metabolism and sleep and wakefulness behaviors. Female C57BL/6 mice are leaner, are more resistant to diet-induced obesity, and spend a longer amount of time in wakefulness than male mice (Funato et al., 2009, 2016). Interestingly, the body weight of male *Ptf1a* cKO mice was similar to that of the male control littermate mice, whereas the body weight of female *Ptf1a* cKO mice was higher than that of female controls, resulting in no significant difference in body weight between sexes in *Ptf1a* cKO mice (Figure S5A). The energy expenditure of female *Ptf1a* cKO mice was significantly lower than that of female control mice, whereas the energy expenditure of male *Ptf1a* cKO mice was similar to that of control mice (Figure S5B). The daily food intake of *Ptf1a* cKO mice was similar to that of control mice in both sexes (Figure S5C). When fed a high-fat diet (HFD), female *Ptf1a* cKO mice gained more weight than female control mice (Figure S5D). In contrast, the weight gain of male *Ptf1a* cKO mice on the HFD was similar to that of control mice (Figure S5D). The HFD intake of *Ptf1a* cKO mice was similar to that of control mice in both sexes (Figure S5E). Cold exposure resulted in a larger decrease in body temperature of female *Ptf1a* cKO mice than female control mice, although the body temperature of male *Ptf1a* cKO and control mice was stable in the cold condition (Figure S5F).

Time spent in wakefulness, non-rapid eye movement (NREM) sleep and rapid eye movement (REM) sleep of *Ptf1a* cKO mice was similar to that of control mice in both sexes (Figure S5G). However, for control mice, the total wake time of female mice was longer than that of male mice, whereas *Ptf1a* cKO mice did not show a sex difference in the total wake time (Figure S5G).

Altered Sex-Biased Gene Expression in the *Ptf1a*-Deficient Mice

Because both male and female *Ptf1a* cKO mice did not demonstrate sexual behaviors in response to gonadal hormones, we examined whether masculinization and feminization were disrupted in *Ptf1a* cKO adult brains using Kiss1, tyrosine hydroxylase (TH), calbindin, and estrogen receptor alpha (Esr1), as these genes are expressed in a sex-biased manner. *Kiss1* is expressed in and around the ARH and AVPV, where the numbers of Kiss1-positive cells are higher in female than male mice (Poling and Kauffman, 2013). Surprisingly, the numbers of *Kiss1*-positive neurons in the AVPV and ARH were both dramatically lower in *Ptf1a* cKO mice than in control mice in both sexes (Figures 5A and 5B). In particular, *Kiss1*-positive neurons in the ARH were clearly lacking in *Ptf1a* cKO mice (Figure 5B), despite no changes in the number of *Npy*- or *Pomc*-expressing neurons in the ARH (Figures 5C and 5D).

The number of TH-expressing cells in the female AVPV is normally greater than that in male mice (Semaan and Kauffman, 2010; Scott et al., 2015). However, the number of TH-positive cells in female *Ptf1a* cKO AVPV was decreased to levels similar to that in male control and *Ptf1a* cKO mice (Figure 5E). Similarly, in wild-type mice, males have a larger number of calbindin-positive cells in the sexually dimorphic nucleus of the preoptic area (SDN-POA) than females (Tsuneoka et al., 2017), whereas *Ptf1a* cKO mice did not show a male-biased cell number difference between the sexes (Figure 5F). Although Esr1-positive cells in the MPOA are more abundant in females than in males (Yokosuka et al., 1997), *Ptf1a* cKO mice did not exhibit a significant difference between sexes, because of the increased number of Esr1-positive cells in males and decreased number of Esr1-positive cells in females (Figure 5G). Similarly, Esr1-positive cell number in the ventrolateral part of the VMH (VMHvl) was much higher in the mutant males than in control males (Figure 5H). We did not detect any overt morphological changes in the hypothalamus (Figure S5H) or the size of the pituitary glands (data not shown) in either sex, consistent with the lack of significant changes in the number of *Ptf1a*-lineage and apoptotic cells in *Ptf1a*-null mice at E18.5 (Figures S3D and S3E). By qPCR analysis, we detected no appreciable changes in the *Ptf1a* cKO hypothalamus, except for *Kiss1* (Figure S5I).

Because Kiss1 deficiency causes dysplasia of male and female genital organs (d'Anglemont de Tassigny et al., 2007; Uenoyama et al., 2015), similar to what we observed in adult hypothalamic *Ptf1a*-deficient mice, we examined Kiss1-positive neurons in *Ptf1a*-null mice at embryonic stages. In general, Kiss1 neurons in the ARH appear around E13.5, while Kiss1 neurons in the AVPV do not appear until P10 (Knoll et al., 2013; Semaan et al., 2013; Sanz et al., 2015). At E14.5 and E18.5, the number of *Kiss1*-positive cells in the future ARH region was drastically lower in *Ptf1a*-null embryos compared with controls regardless of sex (Figures 5I–5L). These findings demonstrate that hypothalamic *Ptf1a* is required for the development of *Kiss1*-expressing neurons.

(H) Rates of maternal behavior were scored in virgin control (n = 8) and *Ptf1a* cKO (n = 5) female mice. Tests were repeated three times. Two-way ANOVA followed by Bonferroni's test.

(I and J) Retrieving (I) and grouping (J) behavior rates were averaged from three trials and scored in control (n = 8) and *Ptf1a* cKO (n = 5). Student's t test.

(K) Lordosis reflex rates toward male mounting scored for ovariectomized and hormonally primed *Ptf1a* cKO (n = 5) and control (n = 8) female mice. Student's t test.

Data are expressed as mean ± SEM. *p < 0.05, **p < 0.01, and ***p < 0.001. In (C) and (D), each individual circle value is a mean of two independent biological replicates. In (I)–(K), each circle value is a mean of three independent replicates. See also Figures S4 and S5.

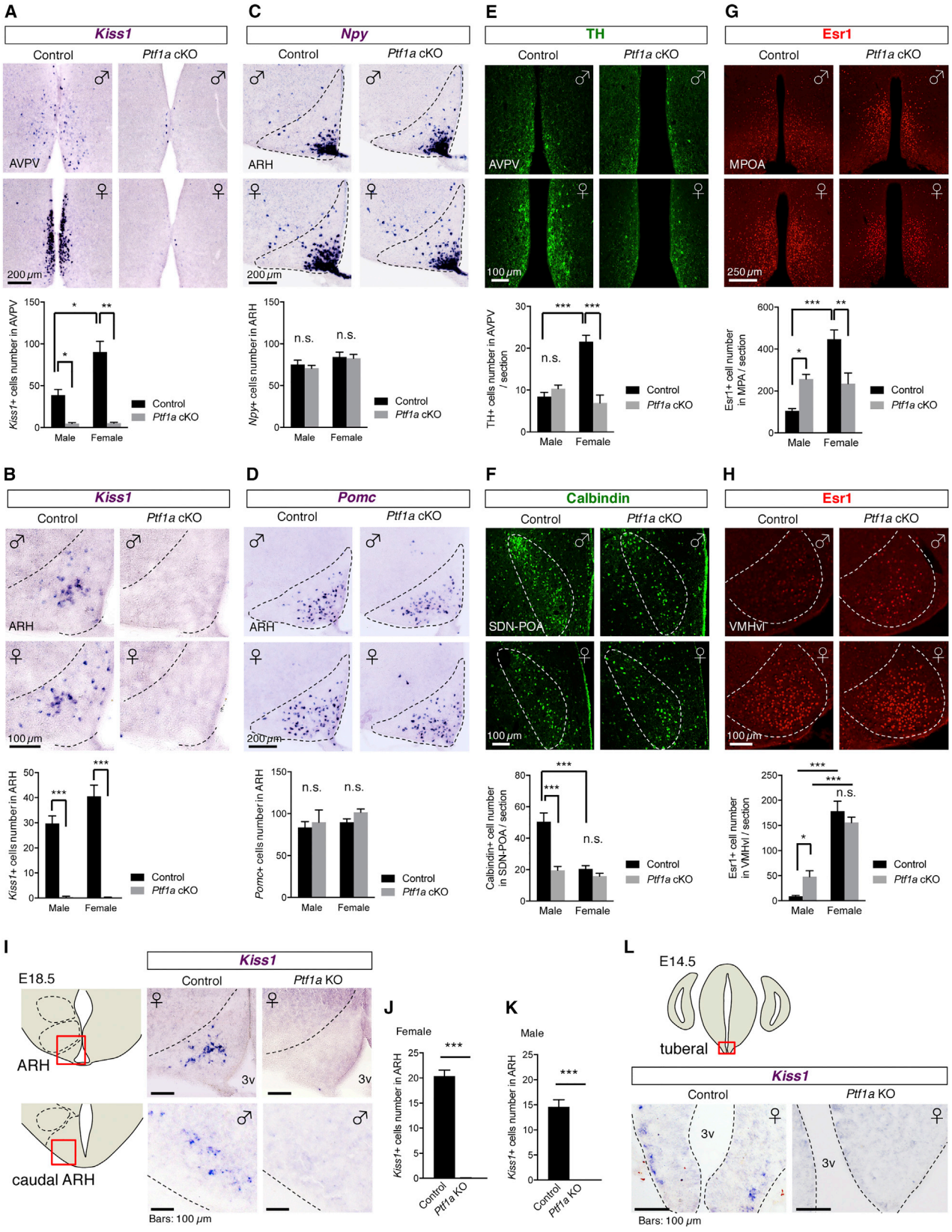

(legend on next page)

Gonadal Development Is Not Impaired in *Ptf1a*-Null Embryos

Next, we examined the reproductive organs in *Ptf1a*-null mice at E18.5. Interestingly, the appearance of testes and ovaries in *Ptf1a*-null embryos was grossly normal at E18.5 (Figures S6A and S6B). Immunostaining for 3β-HSD in the *Ptf1a*-null testis did not reveal an overt change in Leydig cell development at E18.5 (Figure S6C). Hypothalamic *Pgr* mRNA levels reflecting recent testosterone exposure at perinatal stages (Poling and Kauffman, 2012) appeared normal in AVPV and VMHvl of E18.5 *Ptf1a*-null males (Figure S6D). These findings suggest that gonadal structure and function are not strongly affected at embryonic stages in *Ptf1a*-null mice.

Ptf1a-Lineage Cells in Sex-Biased Cell Populations

We subsequently examined how *Ptf1a*-lineage cells are associated with sex-biased cell populations in the hypothalamus using $Ptf1a^{cre/+}$; $Rosa26^{LacZ}$ and $Ptf1a^{cre/+}$; $Rosa26^{tdTomato}$ mice. We found that the majority of *Kiss1*-positive neurons in the AVPV and ARH were not of the *Ptf1a*-lineage in both males and females (6.2 ± 3.6% and 9.6 ± 3.3% in AVPV, 1.9 ± 1.9% and 5.5 ± 3.4% in ARH; Figures 6A–6F). Similarly, most TH-positive cells in the AVPV and ARH and calbindin-positive cells in the SDN-POA did not arise from the *Ptf1a* lineage (Figures 6G–6I). However, a small population of Esr1-positive cells were of *Ptf1a* lineage in the MPOA (male, 13.0 ± 1.1%; female, 19.9 ± 1.8%; Figures 6J, 6K, and 6N) and in the VMHvl (male, 5.4 ± 1.1%; female, 17.4 ± 2.9%; Figures 6L, 6M, and 6O). The ratios of Esr1-positive cells in *Ptf1a*-lineage cells in both the MPOA and VMHvl in females were higher than those in male mice (Figures 6N and 6O). GnRH-positive cells in the POA were not observed in *Ptf1a*-lineage cells (Figure 6P).

RNA-Seq Analysis of Hypothalamic *Ptf1a*-Lineage Cells

Because Ptf1a is a transcription factor, this protein should regulate transcription of various genes in *Ptf1a*-expressing cells of the hypothalamus. To detect those downstream genes, we purified cells in the *Ptf1a* lineage from the hypothalamus at E14.5 by FACS, subsequently performed RNA-seq analysis, and obtained 706 differentially expressed genes (Figure 7A). Three hundred eighty-six genes had lower and 320 had higher expression in *Ptf1a*-lineage cells from homozygous *Ptf1a*-deficient mice (Figures 7B; Table S2). The downregulated genes included *Prdm13*, *Corl2*, and *Lhx5*, which are known downstream targets of *Ptf1a*, as well as *Sox3* and *Nkx2-1*, which are known to be required for hypothalamic development. Interestingly, among those affected genes, we detected several genes encoding transmembrane and/or secreted proteins, such as *Jag2* (ligand for Notch receptors), *Sema6b*, and *Sema4g* (ligands for Plexin family proteins) (Figures 7C and 7D). These genes may have a non-cell-autonomous role in the sexual differentiation of hypothalamic cells adjacent to *Ptf1a*-lineage cells (Figure 7E). *Kiss1* expression was not altered, as was expected by the finding that most *Kiss1*-expressing cells were not in the *Ptf1a* lineage.

DISCUSSION

Ptf1a Is Expressed and Functions in the Embryonic Hypothalamus

In the present study, we showed that Ptf1a was expressed in the neuroepithelial cells and immature neurons in or near the ventricular zone of the preoptic and tuberal regions of the forebrain at mid-embryonic stages (E10.5–E16.5). *Ptf1a*-lineage cells were abundantly found in the ARH and VMH, which is consistent with the finding that the ARH and VMH are derived from the ventricular zone that expresses Rax and Nkx2.1 (Xie and Dorsky, 2017), where Ptf1a is expressed at E12.5. A small number of *Ptf1a*-lineage cells were also found in the DMH, lateral hypothalamic area, median eminence, and medial tuberal nucleus, but not in the paraventricular hypothalamic nucleus, suprachiasmatic nucleus, or anterior hypothalamus. In contrast to the restricted fate of *Ptf1a*-lineage cells in the cerebellum, cochlear nucleus, spinal cord, and retina into inhibitory neurons (Glasgow et al., 2005; Hoshino et al., 2005; Fujitani et al., 2006; Fujiyama et al., 2009), forebrain *Ptf1a*-lineage cells develop into a variety of neuronal subtypes, such as glutamatergic, GABAergic, dopaminergic, and peptidergic cells. Because forebrain *Ptf1a* deficiency disturbed the formation of sexually biased gene expression in the hypothalamus, *Ptf1a* expression in the hypothalamus is required for sexual differentiation of the brain.

Previous studies have demonstrated that *Ptf1a* deficiency causes aberrant migration, cell death, and altered fate transition of *Ptf1a*-lineage cells in the hindbrain, spinal cord, and retina (Glasgow et al., 2005; Hoshino et al., 2005; Fujitani et al., 2006; Yamada et al., 2007; Fujiyama et al., 2009). However, our present study shows that forebrain *Ptf1a* deficiency does not alter the distribution or number of *Ptf1a* lineage cells nor the gross hypothalamic structure in adulthood, suggesting that hypothalamic *Ptf1a* might not contribute to the migration or survival of neurons. The fate transition of *Ptf1a*-lineage cells from glutamatergic to GABAergic neurons was not observed in the VMH in *Ptf1a*-null embryos. Thus, hypothalamic *Ptf1a* may not be involved in the excitatory versus inhibitory determination.

Figure 5. Histological Analysis of *Ptf1a* cKO Mutant Mice Reveals Sex Difference Changes in Hypothalamic Gene Expression

(A–D) *In situ* hybridization with *Kiss1* (A and B), *Npy* (C) and *Pomc* (D) in the indicated regions (AVPV and ARH) of adult control and *Ptf1a* cKO mice. Sexes are indicated. Quantification of positive cells is shown in graphs (n = 3 mice per group).

(E–H) Immunostaining with indicated antibodies in the indicated hypothalamic regions (AVPV, SDN-POA, MPOA, and VMHvl) of adult control and *Ptf1a* cKO mice. Sexes are indicated. Quantification of positive cells is shown in graphs (n = 5 mice per group). Two-way ANOVA followed by Tukey's test (E and F) and Newman-Keuls's test (G and H).

(I) *Kiss1* mRNA expression in ARH of $Ptf1a^{cre/+}$ and $Ptf1a^{cre/cre}$ embryos at E18.5. Schematic of hypothalamic regions and representative images are shown.

(J and K) Quantification of *Kiss1*-positive cells at E18.5 (n = 3 mice per group) in female (J) and male (K) mice. Student's t test.

(L) *Kiss1*-positive cells in prospective ARH of $Ptf1a^{cre/+}$ and $Ptf1a^{cre/cre}$ mice at E14.5. Schematic of tuberal diencephalon and representative images are shown.

Data are expressed as mean ± SEM. *p < 0.05, **p < 0.01, and ***p < 0.001. See also Figure S6.

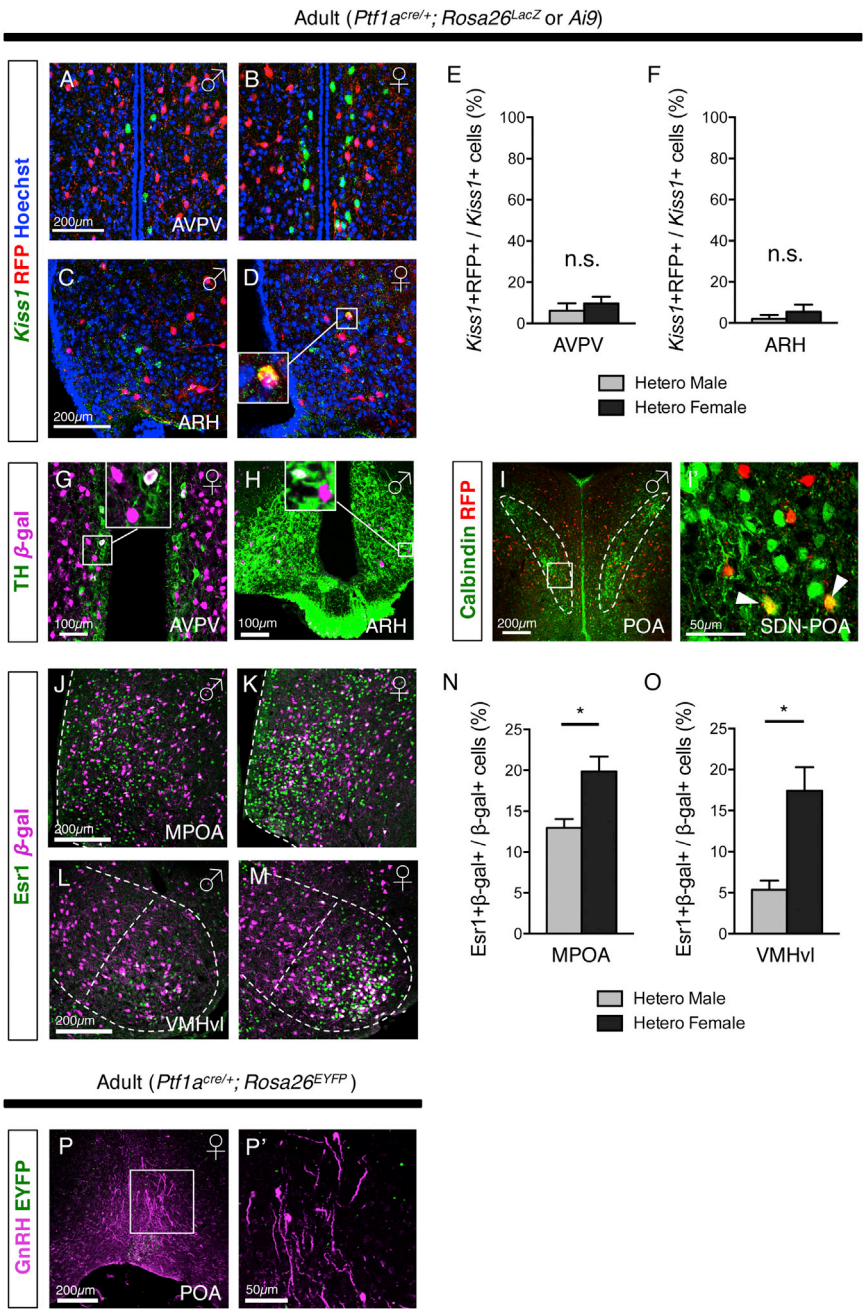

Figure 6. Examination of Sex-Biased Cells in Hypothalamic *Ptf1a*-Lineage Cells

(A–D) Double staining for RFP immunohistochemistry and *Kiss1* ISH in coronal sections of adult *Ptf1a*$^{cre/+}$; *Ai9* male (left) and female (right) mice. Upper panels show AVPV (A and B), and lower panels show ARH (C and D). Inset in (D) is magnified image of double-labeled cell. Hoechst was used to stain nuclei.

(E and F) The percentages of RFP-positive cells in *Kiss1*-positive neurons (n = 4 mice) in the AVPV (E) and ARH (F). Student's t test.

(G and H) Double immunostaining for TH with β-gal in the AVPV (G) and ARH (H) of *Ptf1a*$^{cre/+}$; *Rosa26*^{lacZ} mice. Insets are magnified views of boxed region.

(I and I′) Double immunolabeling of calbindin with β-gal in SDN-POA of male mice. Most calbindin-positive cells in the SDN-POA were negative for β-gal. Magnified view of boxed region in (I) is shown in (I′). A few co-labeled cells were observed (arrowheads).

(J–M) Double immunohistochemistry for Esr1 and β-gal in MPOA (top) and VMHvl (bottom).

(N and O) The percentages of β-gal-positive cells in Esr1-positive neurons (n = 4 mice) in the MPOA (N) and VMHvl (O). Student's t test.

(P and P′) GnRH neurons were not in *Ptf1a* lineage. Sections from adult *Ptf1a*$^{cre/+}$; *Rosa26*^{EYFP} mice. Magnified view of boxed region is shown in (P′).

Scale bars in (A)–(D), (I), (J)–(M), and (P), 200 μm; scale bars in (G) and (H), 100 μm; scale bars in (I′) and (P′), 50 μm. Data are expressed as mean ± SEM. n.s., not significant; *p < 0.05.

Kiss1-Dependent Phenotypes in the Forebrain *Ptf1a*-Deficient Mice

The earliest change we found in mice deficient in forebrain *Ptf1a* was the lack of *Kiss1* expression in the ARH at E14.5, which continued into adulthood. *Kiss1* expression was also lost in adult AVPV in those mice. Previous reports have suggested that kisspeptin-GPR54 signaling plays an important role in brain sexual development (Kauffman et al., 2007; Nakamura et al., 2016). This leads to the notion that part of the phenotypes observed in the forebrain *Ptf1a*-deficient mice may be caused by loss of *Kiss1* expression in the hypothalamus. Actually, some phenotypes of forebrain *Ptf1a*-deficient mice resemble those in rodents deficient in kisspeptin and its receptor, GPR54, and therefore, those can be regarded as *Kiss1*-dependent phenotypes. On the other hand, we also found phenotypes in forebrain *Ptf1a*-deficient mice that have not been observed in *Kiss1*- and/or *Gpr54*-deficient animals (*Kiss1*-independent phenotypes).

At the adult stage, *Kiss1*- and/or *Gpr54*-deficient male animals are viable but infertile, do not display spermatogenesis, and have low testosterone, undescended testes, and scant Leydig cells (d'Anglemont de Tassigny et al., 2007; Kauffman et al., 2007; Uenoyama et al., 2015). *Kiss1*- and/or *Gpr54*-deficicent female mice have a thin uterus and do not show a vaginal opening, an estrous cycle, or corpora lutea in the ovary (d'Anglemont de Tassigny et al., 2007; Lapatto et al., 2007; Uenoyama et al., 2015). These abnormalities were also observed in the forebrain *Ptf1a*-deficient adult mice, which suggests that *Kiss1* expression, regulated by Ptf1a, is required for the establishment of sex hormonal milieu and sex organs in adults. However, at the perinatal stages, testosterone levels are normal in both *Kiss1*- and *Gpr54*-deficient animals

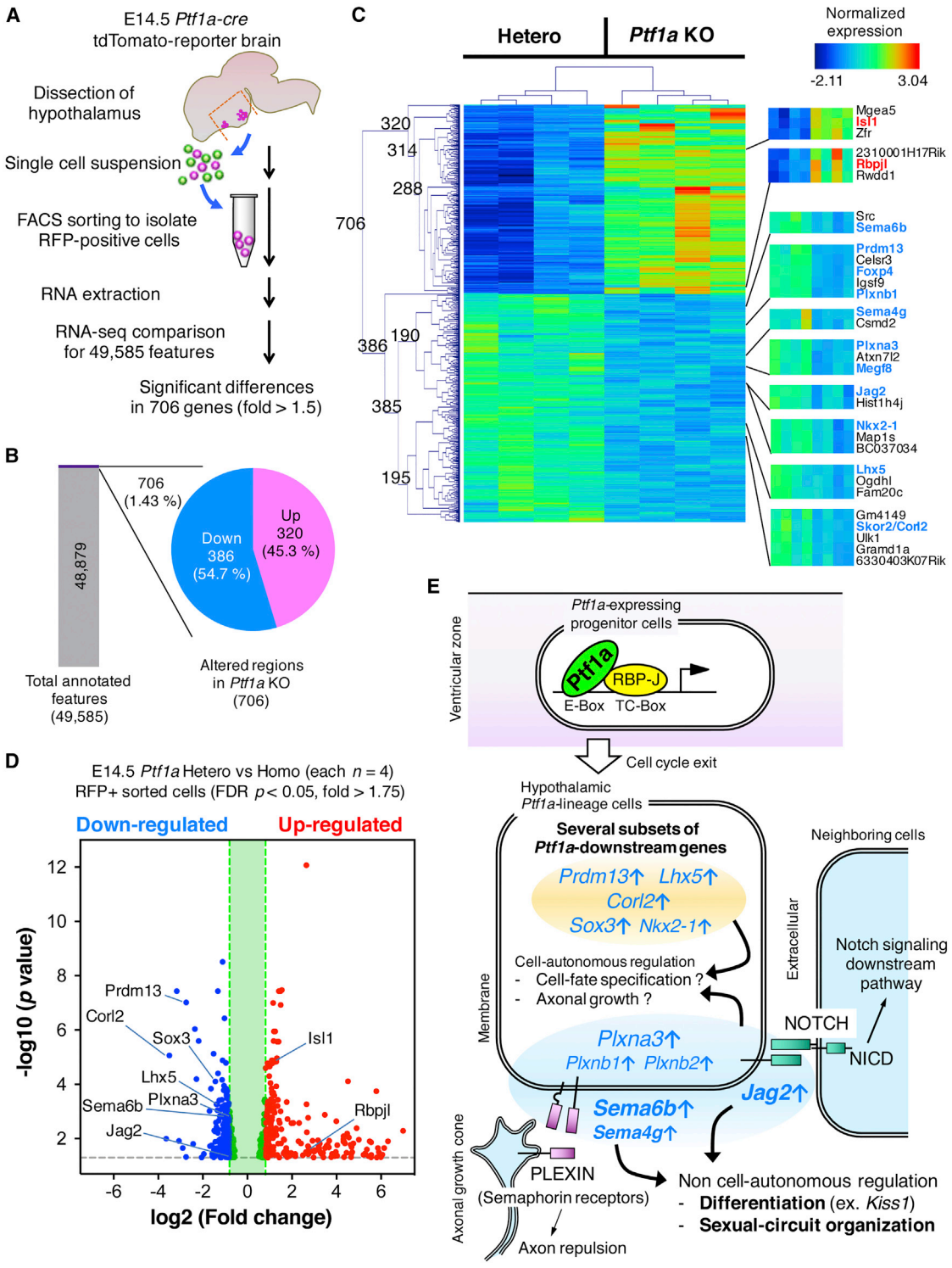

Figure 7. RNA-Seq Analysis of E14.5 Hypothalamic *Ptf1a*-Lineage Cells

Gene expression analysis by RNA-seq demonstrates dysregulation of multiple genes associated with non-cell-autonomous regulation.

(A) Schematic processes of brain dissection, cell suspension, FACS, and RNA-seq. E14.5 *Ptf1a* heterozygotes (*Ptf1a*$^{cre/+}$; *Ai9*) and homozygotes (*Ptf1a*$^{cre/cre}$; *Ai9*) were used (each n = 4 independent embryos). RFP-positive cells from POA and ventral hypothalamus were intermingled. RNA-seq comparison was performed in 49,585 features annotated in mouse GENCODE (GRCm38/mm10) that included transcript variants.

(B) Rates in differentially expressed regions. The majority of variation-exhibiting genes were downregulated in cells from *Ptf1a*-KO mice.

(legend continued on next page)

(Poling and Kauffman, 2012; Nakamura et al., 2016). Similarly, Leydig cells and hypothalamic *Pgr* levels (an indicator of androgen exposure) were normal in *Ptf1a*-null animals at the perinatal stage, although at the adult stage, Leydig cells were severely reduced. These observations suggest that kisspeptin signaling is required for sex organ development, putatively after the perinatal critical period of brain sex differentiation. Note that fetal Leydig cells are thought to be a population distinct from adult Leydig cells (Wen et al., 2016), which *Ptf1a* cKO mice lack in adulthood. Prior to puberty, the luteinizing hormone increases and subsequently induces the proliferation and maturation of adult Leydig cells (Svechnikov et al., 2010; Svingen and Koopman, 2013). Thus, development of adult Leydig cells may be dependent on the proper maturation of the HPG axis (d'Anglemont de Tassigny and Colledge, 2010) in which kisspeptin is involved.

No brain masculinization was observed in male forebrain *Ptf1a*-deficient mice. The supplementation of testosterone failed to induce male sexual behavior in forebrain *Ptf1a*-deficient mice. Forebrain *Ptf1a*-deficient mice also failed to show a male-biased increase in the number of calbindin-positive cells in the SDN-POA. These behavioral and morphological phenotypes of forebrain *Ptf1a*-deficient mice are also found in *Kiss1*-deficient rodents. *Kiss1*-deficient rats failed to exhibit male sexual behaviors in response to exogenous testosterone and lacked a male-type SDN-POA (Nakamura et al., 2016). Brain masculinization is induced by a perinatal testosterone surge at the critical period (Poling and Kauffman, 2013; Yang and Shah, 2014). Fetal Leydig cells secrete testosterone independent of the luteinizing hormone secreted from the pituitary (Wen et al., 2016). It has been shown that male *Kiss1*/*Gpr54* mutant animals have normal androgen milieu at perinatal stages, and their brains are exposed to testosterone at the critical period (Kauffman et al., 2007; Nakamura et al., 2016). Similarly, *Ptf1a* KO brains seemed to receive testosterone at the period, because we observed *Pgr* expression in *Ptf1a* KO hypothalamus at E18.5. These observations indicate that the male brains of *Ptf1a*/*Kiss1*/*Gpr54* mutants receive perinatal testosterone surge but cannot undergo masculinization and further suggest that kisspeptin signaling confers differentiation capability of the brain when exposed to testosterone at the critical period.

Recently, Clarkson et al. raised the possibility that neonatal testosterone surge may be governed by luteinizing hormone secreted from GnRH neurons within a narrow time window as narrow as several hours (Clarkson and Herbison, 2016). Temporal expression of Kiss1 in the AVPV may be responsible for neonatal testosterone surge (Clarkson et al., 2014). If this hypothesis is true, reduced perinatal *Kiss1* expression in the AVPV in forebrain *Ptf1a*-deficient mice may result in suppressed neonatal testosterone surge and subsequently suppress brain masculinization.

In addition, female-specific obesity observed in the hypothalamic *Ptf1a*-deficient mice was also replicated in *Gpr54*-deficient mice (Tolson et al., 2014), presumably caused by decreased energy expenditure. This suggests Ptf1a and kisspeptin signaling may somehow regulate metabolism of animals.

Kiss1-Independent Phenotypes in *Ptf1a* cKO Mice

Forebrain *Ptf1*-deficient mice also exhibited several phenotypes that are not observed in *Gpr54*-deficient animals. Female *Gpr54*-deficient mice exhibited lordosis reflex (Kauffman et al., 2007), whereas female forebrain *Ptf1* cKO mice did not. In the AVPV, female *Gpr54*-deficient mice had a normal number of TH-positive cells (Kauffman et al., 2007), while female *Ptf1a* cKO mice had a decreased number of TH-positive cells. Because TH-positive cells in the AVPV are reported to promote maternal behavior (Scott et al., 2015), decreased TH-positive cells may cause suppressed maternal behaviors in female *Ptf1a* cKO mice. Thus, hypothalamic *Ptf1a* may be required for gene expression and formation of neural circuits that induce female sexual and maternal behavior, independent of *Kiss1*. Furthermore, it is also suggested that feminization of female brains does not automatically occur by non-exposure of testosterone at the critical period, but it requires *Ptf1a* function in the embryonic hypothalamus.

A Machinery whereby Hypothalamic *Ptf1a* Regulates Sexual Differentiation of the Brain

As described above, brain feminization does not automatically occur by non-exposure of testosterone at the critical period in the *Ptf1a* cKO females. Similarly, brain masculinization does not occur in the *Ptf1a* cKO males, although they are exposed to testosterone at the critical period, which is shown by hypothalamic *Pgr* expression at the period. These findings suggest that the *Ptf1a* cKO brains do not respond to testosterone-exposure and non-exposure signals for masculinization and feminization, respectively, and further suggest that Ptf1a confers the competence to respond to such signals on the brain. Because Ptf1a is expressed from E10.5 to E16.5, brains acquire this "sex differentiation competence" during this embryonic period under the control of Ptf1a.

Among previously identified molecules involved in brain sex differentiation, Ptf1a seems to be the earliest regulator that is expressed in progenitors and immature neurons in or near the ventricular zone, at the stage much prior to the critical period. A part of the machinery can be explained by loss of *Kiss1* expression in the hypothalamus. Because the majority of Kiss1 neurons are not in the *Ptf1a* lineage, Ptf1a may be required for the development

(C) Clustered heatmap showing expression status on the basis of intrinsically altered expressions over 1.5-fold. Clusters are generated by Pearson's correlation and average linkage analysis of unsupervised data. Several noteworthy gene symbols exhibiting up (red) and down (blue) are magnified.
(D) Volcano plot with differential expressions for all genes between hetero and homo RFP^+ cells ($p < 0.05$). Dots to the left of zero represent genes with higher expression in cells from heterozygous, and those to the right represent genes with higher expression in cells from homozygous. Dots in the middle region (green) represent genes exhibiting changes under 1.75-fold.
(E) A possible hypothetical model for cell and non-cell-autonomous effects of hypothalamic Ptf1a. A part of diencephalic neural circuit formation may be regulated by the semaphorin family (Funato et al., 2000). Notch signaling may be required for Kiss1 neuron development (Biehl and Raetzman, 2015).
See also Table S2.

of Kiss1 neurons in the developing ARH in a cell lineage-non-autonomous manner.

One possible explanation is that *Ptf1a*-lineage cells induce neighboring non-*Ptf1a*-lineage cells to differentiate into Kiss1 neurons via transmembrane and/or secreted proteins whose expression is reduced (or increased) in *Ptf1a*-deficient-lineage cells (Figure 7E). Because Jag2 (a ligand for Notch) is among the affected genes, one possibility is that Notch signaling may account for the cell-non-autonomous effect. For example, mice deficient in *Rbpj*, which mediates both Ptf1a-dependent and Notch-dependent gene expression, lack Kiss1 neurons but have Pomc neurons in the ARH (Biehl and Raetzman, 2015). Additionally, Ptf1a works as a crucial activator of a Notch ligand, Dll1, in pancreatic progenitor cells (Ahnfelt-Rønne et al., 2012). On the other hand, we also detected several downregulated genes, including signaling molecules in the Semaphorin-Plexin pathway, which might participate in hypothalamic sexual neuronal circuit formation.

As the expression of *Kiss1* in AVPV is detected as early as P10 (Semaan et al., 2013), the molecular nature of *Ptf1a*-lineage cells in the AVPV may be altered at postnatal stages. Postnatal *Kiss1* expression in the AVPV may be affected in a cell-non-autonomous manner by *Ptf1a* deficiency. Further experiments are required to test these possibilities.

As to the *Kiss1*-independent phenotypes, we do not know currently how the *Ptf1a* deficiency causes those abnormalities. However, we detected many genes whose expression was altered in *Ptf1a*-deficient-lineage cells at E14.5. We believe that some of those genes may be involved in sexual development of the brain and account for *Kiss1*-inependent phenotypes.

In this study, we showed that Ptf1a is expressed in the hypothalamus at mid-embryonic stages and involved in sexual development of male and female brains in both *Kiss1*-dependent and *Kiss1*-independent manners. Further studies will be required to fully understand the machinery for sex development of the brains.

EXPERIMENTAL PROCEDURES

Further details and an outline of resources used in this study can be found in Supplemental Experimental Procedures.

Experimental Animals

The mouse lines used in this study are listed in Table S3. All mice were backcrossed more than six generations to C57BL/6J. The day of insemination was designated as E0.5. The embryonic gender was determined by *Sry* genotyping. The ages used in each experiment are included in the relevant text, figures, and figure legends. *Ptf1a*^{cre}, *Ptf1a*^{YFP}, *Rosa26*^{LacZ}, and *Gad67*$^{GFP\Delta neo}$ mouse lines were described previously (Burlison et al., 2008; Fujiyama et al., 2009). *Rosa26*^{EYFP} (stock no. 006148), *Ai9* (stock no. 007909), *En1-Cre* (stock no. 007916), and *Nkx2.1-Cre* (stock no. 008661) lines were obtained from The Jackson Laboratory. All animal experiments in this study were approved by the Animal Care and Use Committee of the National Institute of Neuroscience and the guidelines established by the Institutional Animal Care and Use Committee of the University of Tsukuba.

Statistical Analysis

The experiments were done with the observer double blinded to genotypes and treatment assignments. Sample sizes were determined empirically on the basis of standards in the field. All statistical comparisons were performed using Prism 7 software (GraphPad) and are presented as mean ± SEM. Details of each experiment are included in the figure legends (n values and their meanings and statistical tests used). A p value < 0.05 was considered to indicate statistical significance.

DATA AND SOFTWARE AVAILABILITY

The accession number for the RNA-seq data reported in this paper is GEO: GSE112935. See also https://doi.org/10.17632/43cfk6c547.3.

SUPPLEMENTAL INFORMATION

Supplemental Information includes Supplemental Experimental Procedures, six figures, and three tables and can be found with this article online at https://doi.org/10.1016/j.celrep.2018.06.010.

ACKNOWLEDGMENTS

We thank all Hoshino and Y/F lab members for kind support and technical assistance. We are also grateful to Dr. Ruth Yu for her comments; Drs. T. Tanaka, A. Imura, M. Watanabe, T. Shimogori, Y. Sasai, and M. Matsuda for critical suggestions and antibody reagents; and Drs. K. Takase and T. Terashima for helpful advice on histology. M. Yanagisawa was an investigator at the Howard Hughes Medical Institute (HHMI) during the period of this work. This work is supported by Grant-in-Aid for Research Activity Start-Up (24800088 to T.F.), Japan Society for the Promotion of Science (JSPS) Fellows (15J00393 to T.F.), JSPS KAKENHI (26220207 and 17H06095 to M. Yanagisawa and H.F.; 17H04023, 16K15187, and 15H05942 to H.F.), CREST (JPMJCR1655 to M. Yanagisawa), Scientific Research (15H04268 to M.H.), the Funding Program for World-Leading Innovative R&D on Science and Technology (to M. Yanagisawa) from the JSPS, the Strategic Research Program for Brain Sciences (SRPBS) (17dm0107085h0002 to M.H.) of the Japan Agency for Medical Research and Development (AMED), Intramural Research Grants for Neurological and Psychiatric Disorders of the National Center of Neurology and Psychology (NCNP) (27-7, 28-4 to M.H.), Innovative Areas (15H01304, 16H06528 to M.H.; 17H05963 to Y.T.), and World Premier International Research Center Initiative (to M. Yanagisawa) from the Ministry of Education, Culture, Sports, Science and Technology (MEXT) of Japan.

AUTHOR CONTRIBUTIONS

T.F., H.F., and M.H. designed the project. T.F., S.M., M.N., M.K., and S.K. performed all histological and imaging experiments and statistical analysis. T.F., K.K., M.M., A.S., and H.F. coordinated the FACS and RNA-seq experiments. Y.I., S.M., M. Yamashita, and T.O. helped with genetic studies. T.F., Y.T., S.K., and H.F. executed, analyzed, and interpreted all animal behavioral experiments. M.A.M. provided *Ptf1a*^{YFP} mice. Y.Y. provided *Gad67*$^{GFP\Delta Neo}$ mice. Y.K. provided *Ptf1a*^{cre} mice. M. Yanagisawa and H.F. supervised the sleep analysis. Y.N. and M. Yanagisawa co-mentored T.F. during the course of this study. T.F., H.F., and M.H. wrote the manuscript.

DECLARATION OF INTERESTS

The authors declare no competing interests. M.M. is a consultant for Tsukuba i-Laboratory LLP.

Received: August 30, 2017
Revised: February 14, 2018
Accepted: May 31, 2018
Published: July 3, 2018

REFERENCES

Ahnfelt-Rønne, J., Jørgensen, M.C., Klinck, R., Jensen, J.N., Füchtbauer, E.M., Deering, T., MacDonald, R.J., Wright, C.V., Madsen, O.D., and Serup, P. (2012). Ptf1a-mediated control of Dll1 reveals an alternative to the lateral inhibition mechanism. Development *139*, 33–45.

Anderson, D.J. (2016). Circuit modules linking internal states and social behaviour in flies and mice. Nat. Rev. Neurosci. *17*, 692–704.

Bedont, J.L., Newman, E.A., and Blackshaw, S. (2015). Patterning, specification, and differentiation in the developing hypothalamus. Wiley Interdiscip. Rev. Dev. Biol. *4*, 445–468.

Biehl, M.J., and Raetzman, L.T. (2015). Rbpj-κ mediated Notch signaling plays a critical role in development of hypothalamic Kisspeptin neurons. Dev. Biol. *406*, 235–246.

Bonthuis, P.J., Cox, K.H., Searcy, B.T., Kumar, P., Tobet, S., and Rissman, E.F. (2010). Of mice and rats: key species variations in the sexual differentiation of brain and behavior. Front. Neuroendocrinol. *31*, 341–358.

Burlison, J.S., Long, Q., Fujitani, Y., Wright, C.V., and Magnuson, M.A. (2008). Pdx-1 and Ptf1a concurrently determine fate specification of pancreatic multipotent progenitor cells. Dev. Biol. *316*, 74–86.

Clarkson, J., and Herbison, A.E. (2016). Hypothalamic control of the male neonatal testosterone surge. Philos. Trans. R. Soc. Lond. B Biol. Sci. *371*, 20150115.

Clarkson, J., Busby, E.R., Kirilov, M., Schütz, G., Sherwood, N.M., and Herbison, A.E. (2014). Sexual differentiation of the brain requires perinatal kisspeptin-GnRH neuron signaling. J. Neurosci. *34*, 15297–15305.

d'Anglemont de Tassigny, X., and Colledge, W.H. (2010). The role of kisspeptin signaling in reproduction. Physiology (Bethesda) *25*, 207–217.

d'Anglemont de Tassigny, X., Fagg, L.A., Dixon, J.P., Day, K., Leitch, H.G., Hendrick, A.G., Zahn, D., Franceschini, I., Caraty, A., Carlton, M.B., et al. (2007). Hypogonadotropic hypogonadism in mice lacking a functional Kiss1 gene. Proc. Natl. Acad. Sci. U S A *104*, 10714–10719.

Forger, N.G., Strahan, J.A., and Castillo-Ruiz, A. (2016). Cellular and molecular mechanisms of sexual differentiation in the mammalian nervous system. Front. Neuroendocrinol. *40*, 67–86.

Fujitani, Y., Fujitani, S., Luo, H., Qiu, F., Burlison, J., Long, Q., Kawaguchi, Y., Edlund, H., MacDonald, R.J., Furukawa, T., et al. (2006). Ptf1a determines horizontal and amacrine cell fates during mouse retinal development. Development *133*, 4439–4450.

Fujiyama, T., Yamada, M., Terao, M., Terashima, T., Hioki, H., Inoue, Y.U., Inoue, T., Masuyama, N., Obata, K., Yanagawa, Y., et al. (2009). Inhibitory and excitatory subtypes of cochlear nucleus neurons are defined by distinct bHLH transcription factors, Ptf1a and Atoh1. Development *136*, 2049–2058.

Funato, H., Saito-Nakazato, Y., and Takahashi, H. (2000). Axonal growth from the habenular nucleus along the neuromere boundary region of the diencephalon is regulated by semaphorin 3F and netrin-1. Mol. Cell. Neurosci. *16*, 206–220.

Funato, H., Tsai, A.L., Willie, J.T., Kisanuki, Y., Williams, S.C., Sakurai, T., and Yanagisawa, M. (2009). Enhanced orexin receptor-2 signaling prevents diet-induced obesity and improves leptin sensitivity. Cell Metab. *9*, 64–76.

Funato, H., Miyoshi, C., Fujiyama, T., Kanda, T., Sato, M., Wang, Z., Ma, J., Nakane, S., Tomita, J., Ikkyu, A., et al. (2016). Forward-genetics analysis of sleep in randomly mutagenized mice. Nature *539*, 378–383.

Glasgow, S.M., Henke, R.M., Macdonald, R.J., Wright, C.V., and Johnson, J.E. (2005). Ptf1a determines GABAergic over glutamatergic neuronal cell fate in the spinal cord dorsal horn. Development *132*, 5461–5469.

Hoshino, M., Nakamura, S., Mori, K., Kawauchi, T., Terao, M., Nishimura, Y.V., Fukuda, A., Fuse, T., Matsuo, N., Sone, M., et al. (2005). Ptf1a, a bHLH transcriptional gene, defines GABAergic neuronal fates in cerebellum. Neuron *47*, 201–213.

Hossain, M.S., Asano, F., Fujiyama, T., Miyoshi, C., Sato, M., Ikkyu, A., Kanno, S., Hotta, N., Kakizaki, M., Honda, T., et al. (2016). Identification of mutations through dominant screening for obesity using C57BL/6 substrains. Sci. Rep. *6*, 32453.

Kauffman, A.S., Park, J.H., McPhie-Lalmansingh, A.A., Gottsch, M.L., Bodo, C., Hohmann, J.G., Pavlova, M.N., Rohde, A.D., Clifton, D.K., Steiner, R.A., and Rissman, E.F. (2007). The kisspeptin receptor GPR54 is required for sexual differentiation of the brain and behavior. J. Neurosci. *27*, 8826–8835.

Kimmel, R.A., Turnbull, D.H., Blanquet, V., Wurst, W., Loomis, C.A., and Joyner, A.L. (2000). Two lineage boundaries coordinate vertebrate apical ectodermal ridge formation. Genes Dev. *14*, 1377–1389.

Knoll, J.G., Clay, C.M., Bouma, G.J., Henion, T.R., Schwarting, G.A., Millar, R.P., and Tobet, S.A. (2013). Developmental profile and sexually dimorphic expression of kiss1 and kiss1r in the fetal mouse brain. Front. Endocrinol. (Lausanne) *4*, 140.

Lapatto, R., Pallais, J.C., Zhang, D., Chan, Y.M., Mahan, A., Cerrato, F., Le, W.W., Hoffman, G.E., and Seminara, S.B. (2007). Kiss1-/- mice exhibit more variable hypogonadism than Gpr54-/- mice. Endocrinology *148*, 4927–4936.

Lee, B., Lee, S., Lee, S.K., and Lee, J.W. (2016). The LIM-homeobox transcription factor Isl1 plays crucial roles in the development of multiple arcuate nucleus neurons. Development *143*, 3763–3773.

McCarthy, M.M., and Arnold, A.P. (2011). Reframing sexual differentiation of the brain. Nat. Neurosci. *14*, 677–683.

Meredith, D.M., Masui, T., Swift, G.H., MacDonald, R.J., and Johnson, J.E. (2009). Multiple transcriptional mechanisms control Ptf1a levels during neural development including autoregulation by the PTF1-J complex. J. Neurosci. *29*, 11139–11148.

Michaud, J.L., Rosenquist, T., May, N.R., and Fan, C.M. (1998). Development of neuroendocrine lineages requires the bHLH-PAS transcription factor SIM1. Genes Dev. *12*, 3264–3275.

Morales-Delgado, N., Merchan, P., Bardet, S.M., Ferrán, J.L., Puelles, L., and Díaz, C. (2011). Topography of somatostatin gene expression relative to molecular progenitor domains during ontogeny of the mouse hypothalamus. Front. Neuroanat. *5*, 10.

Nakamura, S., Uenoyama, Y., Ikegami, K., Dai, M., Watanabe, Y., Takahashi, C., Hirabayashi, M., Tsukamura, H., and Maeda, K.I. (2016). Neonatal kisspeptin is steroid-independently required for defeminisation and peripubertal kisspeptin-induced testosterone is required for masculinisation of the brain: a behavioural study using Kiss1 knockout rats. J. Neuroendocrinol. *28*, 28.

Poling, M.C., and Kauffman, A.S. (2012). Sexually dimorphic testosterone secretion in prenatal and neonatal mice is independent of kisspeptin-Kiss1r and GnRH signaling. Endocrinology *153*, 782–793.

Poling, M.C., and Kauffman, A.S. (2013). Organizational and activational effects of sex steroids on kisspeptin neuron development. Front. Neuroendocrinol. *34*, 3–17.

Sanz, E., Quintana, A., Deem, J.D., Steiner, R.A., Palmiter, R.D., and McKnight, G.S. (2015). Fertility-regulating Kiss1 neurons arise from hypothalamic POMC-expressing progenitors. J. Neurosci. *35*, 5549–5556.

Scott, N., Prigge, M., Yizhar, O., and Kimchi, T. (2015). A sexually dimorphic hypothalamic circuit controls maternal care and oxytocin secretion. Nature *525*, 519–522.

Semaan, S.J., and Kauffman, A.S. (2010). Sexual differentiation and development of forebrain reproductive circuits. Curr. Opin. Neurobiol. *20*, 424–431.

Semaan, S.J., Tolson, K.P., and Kauffman, A.S. (2013). The development of kisspeptin circuits in the Mammalian brain. Adv. Exp. Med. Biol. *784*, 221–252.

Shimogori, T., Lee, D.A., Miranda-Angulo, A., Yang, Y., Wang, H., Jiang, L., Yoshida, A.C., Kataoka, A., Mashiko, H., Avetisyan, M., et al. (2010). A genomic atlas of mouse hypothalamic development. Nat. Neurosci. *13*, 767–775.

Sternson, S.M. (2013). Hypothalamic survival circuits: blueprints for purposive behaviors. Neuron *77*, 810–824.

Svechnikov, K., Landreh, L., Weisser, J., Izzo, G., Colón, E., Svechnikova, I., and Söder, O. (2010). Origin, development and regulation of human Leydig cells. Horm. Res. Paediatr. *73*, 93–101.

Svingen, T., and Koopman, P. (2013). Building the mammalian testis: origins, differentiation, and assembly of the component cell populations. Genes Dev. *27*, 2409–2426.

Tamamaki, N., Yanagawa, Y., Tomioka, R., Miyazaki, J., Obata, K., and Kaneko, T. (2003). Green fluorescent protein expression and colocalization with

calretinin, parvalbumin, and somatostatin in the GAD67-GFP knock-in mouse. J. Comp. Neurol. *467*, 60–79.

Tolson, K.P., Garcia, C., Yen, S., Simonds, S., Stefanidis, A., Lawrence, A., Smith, J.T., and Kauffman, A.S. (2014). Impaired kisspeptin signaling decreases metabolism and promotes glucose intolerance and obesity. J. Clin. Invest. *124*, 3075–3079.

Tsuneoka, Y., Maruyama, T., Yoshida, S., Nishimori, K., Kato, T., Numan, M., and Kuroda, K.O. (2013). Functional, anatomical, and neurochemical differentiation of medial preoptic area subregions in relation to maternal behavior in the mouse. J. Comp. Neurol. *521*, 1633–1663.

Tsuneoka, Y., Tsukahara, S., Yoshida, S., Takase, K., Oda, S., Kuroda, M., and Funato, H. (2017). Moxd1 is a marker for sexual dimorphism in the medial preoptic area, bed nucleus of the stria terminalis and medial amygdala. Front. Neuroanat. *11*, 26.

Uenoyama, Y., Nakamura, S., Hayakawa, Y., Ikegami, K., Watanabe, Y., Deura, C., Minabe, S., Tomikawa, J., Goto, T., Ieda, N., et al. (2015). Lack of pulse and surge modes and glutamatergic stimulation of luteinising hormone release in Kiss1 knockout rats. J. Neuroendocrinol. *27*, 187–197.

Wen, Q., Cheng, C.Y., and Liu, Y.X. (2016). Development, function and fate of fetal Leydig cells. Semin. Cell Dev. Biol. *59*, 89–98.

Xie, Y., and Dorsky, R.I. (2017). Development of the hypothalamus: conservation, modification and innovation. Development *144*, 1588–1599.

Yamada, M., Terao, M., Terashima, T., Fujiyama, T., Kawaguchi, Y., Nabeshima, Y., and Hoshino, M. (2007). Origin of climbing fiber neurons and their developmental dependence on Ptf1a. J. Neurosci. *27*, 10924–10934.

Yang, C.F., and Shah, N.M. (2014). Representing sex in the brain, one module at a time. Neuron *82*, 261–278.

Yokosuka, M., Okamura, H., and Hayashi, S. (1997). Postnatal development and sex difference in neurons containing estrogen receptor-alpha immunoreactivity in the preoptic brain, the diencephalon, and the amygdala in the rat. J. Comp. Neurol. *389*, 81–93.